

**Fermi National Accelerator Laboratory**

**FERMILAB-Conf-98/060**

## **The Lattice for the 50-50 GeV Muon Collider**

King-Yuen Ng and D. Trbojevic

*Fermi National Accelerator Laboratory  
P.O. Box 500, Batavia, Illinois 60510*

February 1998

Published Proceedings of the *4th International Conference on Physics Potential and Development of Muon Colliders*, San Francisco, California, December 10-12, 1997

Operated by Universities Research Association Inc. under Contract No. DE-AC02-76CH03000 with the United States Department of Energy

## **Disclaimer**

*This report was prepared as an account of work sponsored by an agency of the United States Government. Neither the United States Government nor any agency thereof, nor any of their employees, makes any warranty, expressed or implied, or assumes any legal liability or responsibility for the accuracy, completeness, or usefulness of any information, apparatus, product, or process disclosed, or represents that its use would not infringe privately owned rights. Reference herein to any specific commercial product, process, or service by trade name, trademark, manufacturer, or otherwise, does not necessarily constitute or imply its endorsement, recommendation, or favoring by the United States Government or any agency thereof. The views and opinions of authors expressed herein do not necessarily state or reflect those of the United States Government or any agency thereof.*

## **Distribution**

*Approved for public release; further dissemination unlimited.*

# The Lattice for the 50-50 GeV Muon Collider

King-Yuen Ng<sup>1</sup> and D. Trbojevic<sup>2</sup>

<sup>1</sup>*Fermi National Accelerator Laboratory,<sup>3</sup> P.O. Box 500, Batavia, IL 60510*

<sup>2</sup>*Brookhaven National Laboratory, P.O. Box 5000, Upton, N.Y. 11973-5000*

**Abstract.** The lattice design of the 50-50 GeV muon collider is presented. Due to the short lifetime of the 50 GeV muons, the ring needs to be as small as possible. The 4 cm low betas in both planes lead to high betatron functions at the focusing quadrupoles and hence large chromaticities, which must be corrected locally. In order to maintain a low rf voltage of around 10 MV, the momentum-compaction factor must be kept to less than  $10^{-2}$ , and therefore the flexible momentum-compaction modules are used in the arcs. The dynamical aperture is larger than 6 to 7 rms beam size for  $\pm 5$  rms momentum offset. Comments are given and modifications are suggested.

## I THE 50 GEV LATTICE

The recently proposed 50-50 GeV muon collider has a luminosity of  $1 \times 10^{33} \text{ cm}^2\text{s}^{-1}$  [1]. To accomplish this, the intense bunches, each containing  $1 \times 10^9$  muons, will have an rms length of 4 cm, which is also chosen as the low betatron functions at the interaction point (IP). To reduce the high background in the detector due to the decay of the muons, a dipole of length 1 m and field 9 T must be placed downstream of the last focusing quadrupole and outside the detector. As a result, it has been suggested that the last focusing quadrupole should be placed 4.5 m from the IP. The rms momentum spread of these muon bunches is estimated to be 0.0010 and the rms normalized emittance  $\epsilon_{N\text{rms}} = 80 \times 10^{-6} \pi\text{m}$ . The transverse excursion of the beam will be large. In addition, to prevent the quenching of the superconducting magnets due to the energy released by the decaying muons, they must be shielded by a 2-cm layer of tungsten. Because of all these, the quadrupoles are required to have rather large aperture, and therefore their field gradients are limited. Due to the above restrictions, the betatron functions in the triplet focusing region will be very high, reaching  $\sim 1550$  m in both transverse planes in our design presented below. High betatron functions bring about high natural chromaticities and local correction by sextupoles will be necessary.

Sample lattices have been designed. One of the designs is shown in Fig. 1 starting from the IP. We see first the background clearing dipole followed by the triplet focusing quadrupoles. The interaction region (IR) stops at about 24 m from the IP and the local correction section begins. The Twiss properties of the 4 correction sextupoles are listed in Table 1. The SX1's are the two horizontal correction sextupoles. They are placed at positions with almost the same betatron functions and dispersion function, and are separated horizontally and vertically by phase advances  $\pi$  so that their nonlinear effect will be confined in the region between the

---

<sup>3</sup>) Operated by the Universities Research Association, Inc., under contract with the U.S. Department of Energy.

**TABLE 1.** Twiss properties of the IR correction sextupoles.

	Distance (m)	Phase Advances		Betatron Functions (m)		Dispersion (m)
		$\nu_x$	$\nu_y$	$\beta_x$	$\beta_y$	
SX2	33.3277	0.52280	0.74952	1.06603	100.00063	2.51592
SX2	57.8132	0.99926	1.24953	1.06338	100.00059	2.51851
SX1	46.5892	0.74950	0.96450	100.00552	0.55826	3.20185
SX1	77.5012	1.24858	1.50666	100.56615	1.06291	3.07869

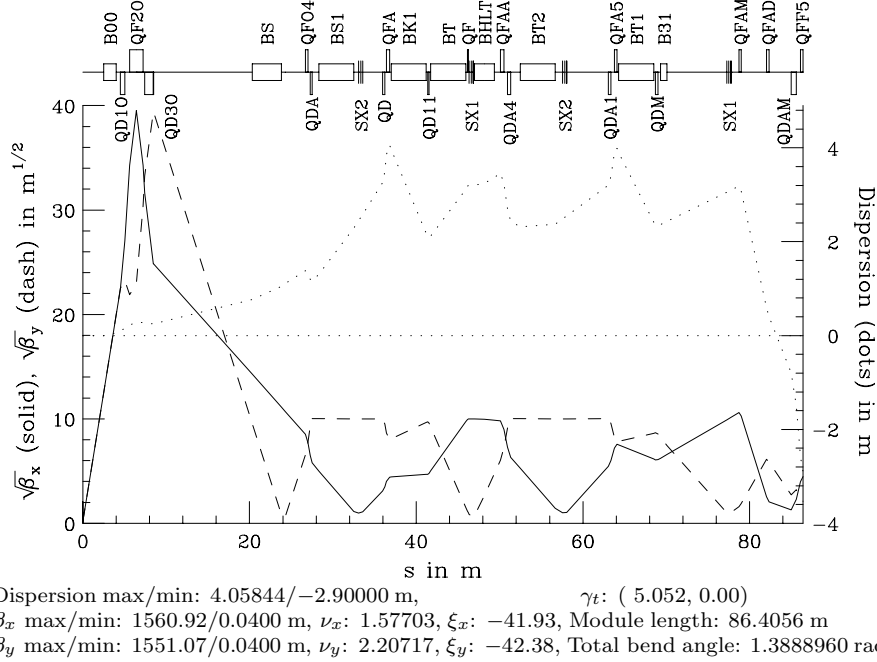
two sextupoles. Their horizontal phase advances are also integral numbers of  $\pi$  from the triplet focusing F-quadrupole so that the chromaticity compensation for that quadrupole will be most efficient [2]. The SX2's are the two vertical correction sextupoles and are placed similarly at designated locations. Notice that the correction section on each side of the IP spans a distance of roughly 62.4 m.

To design the arc section of the collision ring, let us first analyze the possible rf system required. Each muon bunch has an rms length  $\sigma_\ell = 4$  cm and rms momentum offset of  $\sigma_\delta = 0.0010$ . When placed in a matched rf bucket, the synchrotron tune at small amplitude is  $\nu_s = |\eta|\sigma_\delta C / (2\pi\sigma_\ell)$ , where  $\eta$  is the slippage factor and  $C$  is the circumference of the collider ring. The rf voltage required to setup such a bucket will be

$$V_{\text{rf}} = \frac{2\pi E \nu_s^2}{|\eta|h} = \frac{|\eta|E}{2\pi h} \left( \frac{C\sigma_\delta}{\sigma_\ell} \right)^2, \quad (1)$$

where  $h$  is the rf harmonic,  $E$  the muon total energy, and the muon velocity has been taken as the velocity of light. We have the bucket-bunch relation

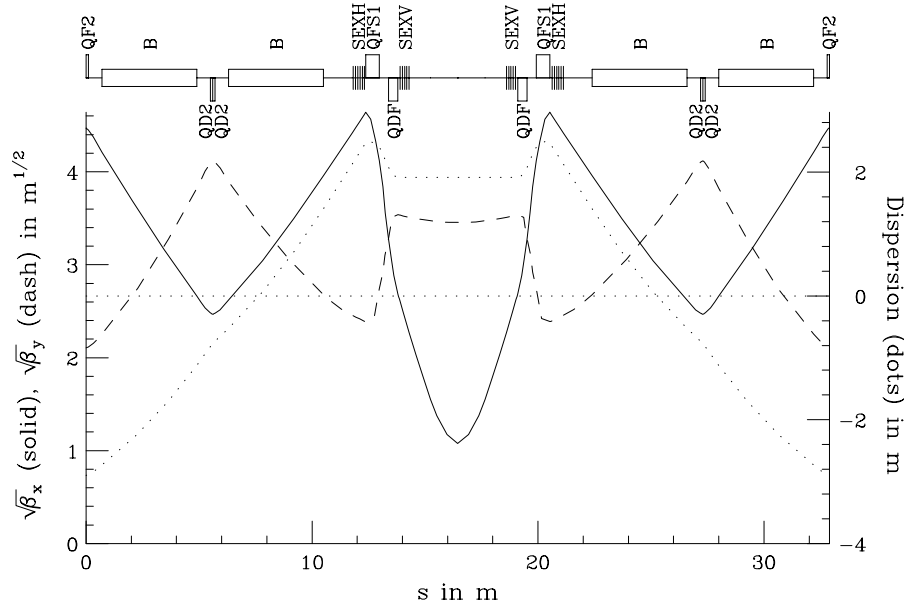
$$\frac{\hat{\delta}}{\sigma_\delta} = \frac{\lambda_{\text{rf}}}{\pi\sigma_\ell} = \frac{C}{\pi h\sigma_\ell}, \quad (2)$$

**FIGURE 1.** The lattice structure of the IR including local chromaticity corrections.

where  $\hat{\delta}$  is the bucket height and  $\lambda_{\text{rf}}$  is the rf wavelength. If we take  $\hat{\delta}/\sigma_{\delta} = 5$  and  $C = 350$  m, one gets  $h = 557$ . Then, from Eq. (1), the rf voltage can be solved as  $V_{\text{rf}} = 1094|\eta|$  MV. In Table 2, the rf voltages corresponding to some possible  $|\eta|$  or transition gammas  $\gamma_t$  are tabulated. It is clear that if we want to have a low rf voltage of around 10 MV, we need to limit the momentum-compaction factor to  $\sim 1 \times 10^{-2}$ . To accomplish that we must use the flexible momentum-compaction (FMC) modules [3] in the arc of the ring. Two such modules will be required for half of the collider ring, one of which is shown in Fig. 2. To close the ring geometrically, there will be a  $\sim 45.1$  m straight section between the two sets of FMC modules. The total length of the collider ring is now only 349.5 m. This is a nice feature, since a small ring allows larger number of collisions before the muons decay appreciably. Note that the IR and local correction sections take up 49.4% of the whole ring.

**TABLE 2.** Relation between  $V_{\text{rf}}$  and slippage factor.

$V_{\text{rf}}$ (MV)	$ \eta $	$\gamma_t$	$\nu_s$
1	0.000914	33.1	0.00127
5	0.00457	14.8	0.00637
10	0.00914	10.5	0.0127
15	0.01371	8.54	0.0191
20	0.01828	7.40	0.0255
25	0.02285	6.62	0.0318
30	0.02742	6.04	0.0382



Dispersion max/min: 2.47014/−2.90000 m,  $\gamma_t$ : ( 0.00, 7.98)  
 $\beta_x$  max/min: 21.52/1.15911 m,  $\nu_x$ : 0.76926,  $\xi_x$ : −1.34, Module length: 32.8999m  
 $\beta_y$  max/min: 16.95/4.43528 m,  $\nu_y$ : 0.58984,  $\xi_y$ : −0.75, Total bend angle: 0.8763483 rad

**FIGURE 2.** Lattice structure of the flexible momentum-compaction module.

## II DYNAMICAL PROPERTIES

### A Dynamical Aperture

Initially 16 particles with the same momentum offset and having vanishing  $x'$  and  $y'$  are placed uniformly on a circle in the  $x$ - $y$  plane. The particles are tracked with the code COSY [4]. The largest radius that provide survival of the 16 particles in 1000 turns is defined here as the dynamical aperture at this momentum offset and is plotted in Fig. 3(a) in units of the rms radius of the beam at the IP. (At the 4 cm low-beta IP, the beam has an rms radius of  $82\text{ }\mu\text{m}$ .) We see that the dynamical aperture is not symmetric in momentum offset. It is about  $7\sigma$  for positive momentum offset, but drops rapidly when the offset becomes negative.

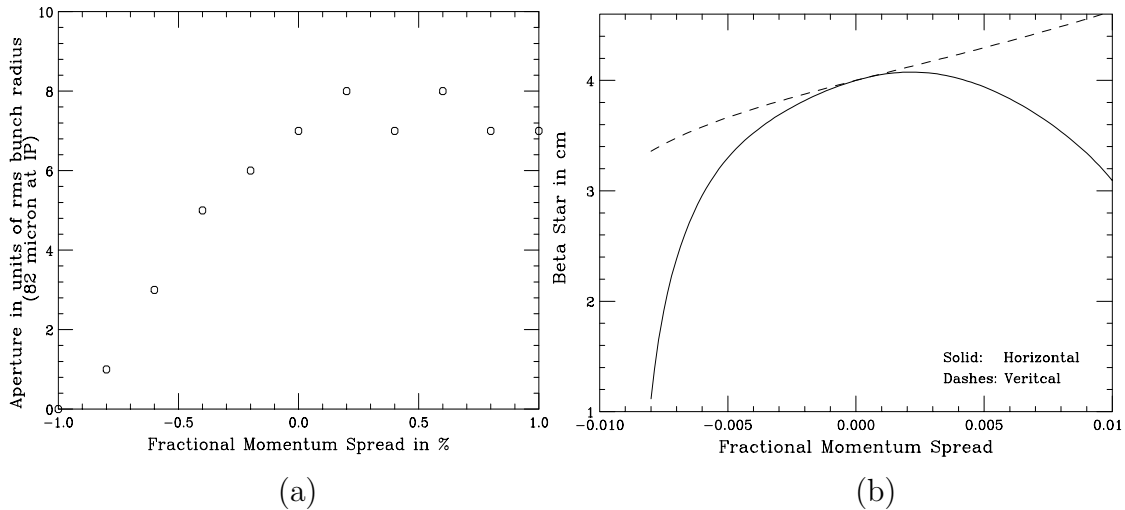


**FIGURE 3.** (a) Dynamical aperture of the lattice versus momentum offset. (b) Betatron functions at the IP versus momentum offset.

### B Betatron Functions at IP with Momentum Offset

We see in Fig. 3(b) that the vertical betatron function at the IP varies almost linearly between  $\sim 3.4$  and  $\sim 4.6$  cm in the range of momentum offset  $-0.008$  and  $+0.010$ . The horizontal betatron function, on the other hand, varies very nonlinearly between  $\sim 1.1$  and  $\sim 4.1$  cm for the same range of momentum offset. This large and rapid variation is an unpleasant feature of the lattice, because it can easily lead to incorrect computation of the luminosity.

### C Tune dependence on Momentum offset

The horizontal and vertical tunes as functions of momentum offset are shown in Fig. 4(a). Although the variation of the vertical tune is small, the variation of the horizontal tune is much larger.

Next we look at the chromaticities of the lattice as functions of momentum offset in Fig. 4(b). Although the chromaticities in both planes have been corrected to

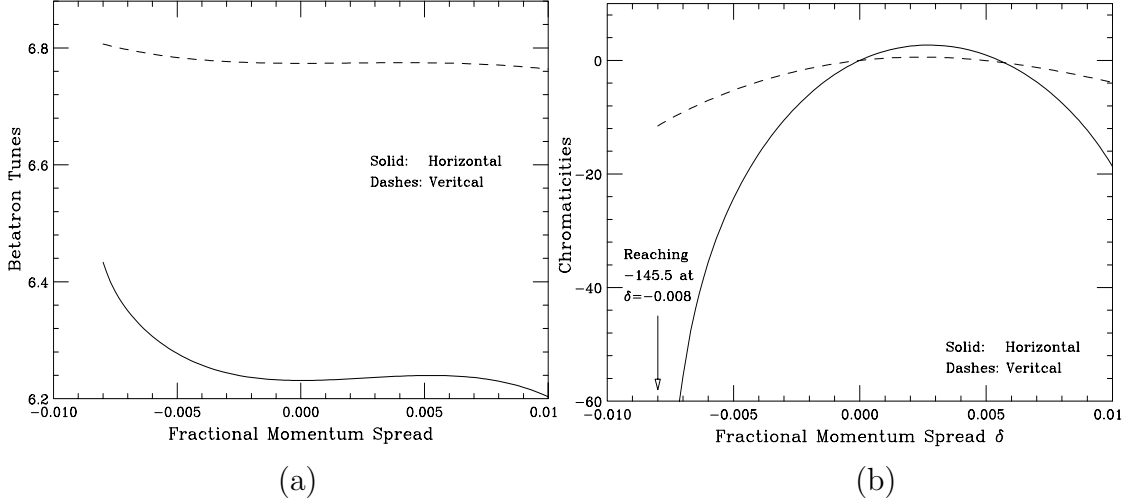


**FIGURE 4.** (a) Horizontal and vertical tunes versus momentum offset. (b) Horizontal and vertical chromaticities versus momentum offset.

zero, the off-momentum variations are still very large, This is especially true for the horizontal variation which decreases extremely fast at negative momentum offsets. We believe this is the culprit that limits the momentum aperture of the lattice. However, not much can be improved, because we have only one family of correction sextupoles in each plane. These sextupoles, SX1 and SX2, are of length 0.5 m and field strengths 281.9 and  $-355.2 \text{ T/m}^2$ , respectively. Considering a 6-cm aperture, the pole tip fields are 1.01 and 1.27 T, respectively. The sextupoles inside the FMC module only correct the much smaller chromaticities of the FMC module, and have little effect on the chromaticities created by the IR. The on-momentum amplitude-dependent tunes of the ring excluding the straight are

$$\begin{aligned}\nu_x &= 6.231 - 2.40 \times 10^2 \epsilon_x - 3.58 \times 10^3 \epsilon_y, \\ \nu_y &= 6.774 - 3.58 \times 10^3 \epsilon_x - 6.65 \times 10^1 \epsilon_y,\end{aligned}\tag{3}$$

where  $\epsilon_x$  and  $\epsilon_y$  are the 95% unnormalized horizontal and vertical emittances measured in  $\pi\text{m}$ . With the designed rms emittances of  $80 \times 10^{-6} \pi\text{m}$ , the 95% unnormalized emittances are  $\epsilon_x = \epsilon_y = 1.014 \times 10^{-6} \pi\text{m}$  (6 times the rms value). Thus the amplitude-dependent tune spreads are only  $< 0.004$  which are small. However, the off-momentum amplitude-dependent tune spreads will be larger due to the larger off-momentum chromaticities.

## D Momentum-Compaction Function

The momentum-compaction factor of the whole ring is  $\alpha_0 = 0.01114$  and varies rather linearly from 0.0082 to 0.013 when the momentum offset changes from  $-0.008$  to  $+0.010$ . To further reduce  $\alpha_0$  to  $\sim 0.001$  and hence the rf voltage in operation to  $V_{\text{rf}} \sim 1 \text{ MV}$ , we must tune the momentum-compaction factor of the FMC module to  $\sim -0.05$ , which is very difficult, requiring high dispersion function and high quadrupole gradients [5]. Note that we have already removed the dipoles at the center of the FMC module in Fig. 2 so as to make the momentum-compaction factor more negative.

### III PROBLEMS WITH THE LATTICE

- (1) What is shown in Fig. 3(a) is the aperture of the *bare* lattice. If we include higher-order field errors, both systematic and random, misalignment errors, synchrotron oscillations, the aperture can be very much reduced. This is a small ring with short magnets and the effects of fringe fields may not be negligible. During the ICFA Frascati Workshop held at Frascati in October of 1997, a lattice for the tau-charm factory was presented by Huang [6]. This machine has a circumference of  $\sim 380$  m. It was pointed out by Koiso that the aperture of the lattice would be very much reduced when fringe fields are included [6]. Therefore, it is very plausible that the momentum aperture of our designed lattice will be reduced to less than  $\pm 5$  rms of momentum offset, when all considerations are included.
- (2) The horizontal chromaticity changes too abruptly in the negative momentum-offset region, which is the source of the small aperture in that region. Therefore, higher-order chromaticities, like beta-beating, etc, must be corrected. However, this is not possible with only one family of sextupoles in each transverse plane.
- (3) Figure 3(b) shows a large variation of the betatron functions at the IP with momentum offset, which is unpleasant. In order to correct for this and higher-order chromaticities, 3 families of sextupoles are required in each transverse plane. Unfortunately, there are only 4 FMC modules in the arc section of ring, and there is not enough space to deploy these sextupoles.

### IV SUGGESTIONS FOR IMPROVEMENT

#### A FODO Cells

If we replace the FMC modules with FODO cells, we will have room to install more sextupoles. The 4 FMC modules together with the 45 m straight amount to a total of  $\sim 177$  m. There, we can install 14 FODO cells each of length 12.6 m and phase advance  $90^\circ$ . Since sextupoles have to be placed  $\pi$  apart to cancel nonlinearity, we can install two more families of sextupoles in each transverse plane. Higher-order chromaticities and the betatron functions at the IP can then be controlled.

The price we need to pay is the more expensive rf system. The horizontal and vertical tunes of the ring will remain about 6 to 8. Since FODO cells are used in the arc region, we expect the transition gamma to be around 6 to 8 as well. According to Table 2, an rf voltage of about 20 to 30 MV will be needed.

#### B Unequal Betatron Functions at IR

Another suggestion is unequal betatron functions at the IP, for example,  $\beta_y^* = 4$  cm, and larger  $\beta_x^*$ . One clear disadvantage is that the luminosity will be reduced almost by half. Also a flat beam will decrease the precision of collision-vertex tagging in the silicon vertex detector. However, there are certainly advantages. First, the final focus can be performed much more easily, since we need to pay attention mostly to the lower  $\beta^*$  only. The chromaticities will be much smaller

and can therefore be corrected easily. Second, hopefully, the chromaticities of the IR are so small that local correction will not be necessary. Notice that in the lattice presented earlier, the two local correction sections take up about  $\sim 36\%$  of the whole ring. If these sections can be eliminated, more FODO cells can be inserted making the 3-family corrections for the chromaticities and  $\beta^*$  dependence on momentum offset more efficient. Moreover, the collider ring can be designed smaller, allowing for more collisions of the muon bunches per unit time, and we will gain back part of the lost luminosity. If the rms length of the muon bunches can be shortened to 3 cm, we can make  $\beta_y^* = 3$  cm and larger for  $\beta_x^*$ . This will also help in gaining back part of the lost luminosity. Finally, the straight section of the lattice presented earlier carries a dispersion up to  $\sim \pm 3$  m. On the other hand, dispersion-free straight section can easily be designed with short FODO cells.

In the following we shall present some elementary designs of the IR and estimate their chromaticities using thin-lens theory. We assume the extreme case of  $\beta_y^* = 4$  cm and  $\beta_x^* = 40$  cm, and use a focusing doublet consisting of quadrupoles of length 1 m each. After the background clearing dipole, the first quadrupole which is defocusing in the  $x$ -plane is centered at 5 m from the IP, and the second quadrupole which is focusing is centered at 6 m. Then at  $s = 5$  m,  $\beta_y \approx s^2/\beta_y^* = 625$  m. Before entering the quadrupole, the *negative-betatron-function-half-slope* is  $\alpha_y = -s/\beta_y^* = -125$ . In order to bend it to  $+125$ , the quadrupole is required to have the integrated strength of  $k = B'\ell/(B\rho) = 2/s = 0.4$  m $^{-1}$ . The field gradient is therefore  $B' = k(B\rho)/\ell = 66.7$  T/m. Taking the rms normalized emittance to be  $\epsilon_{N\text{rms}} = 80 \times 10^{-6}$   $\pi$ m, the  $5\sigma$  beam radius is 5.14 cm. Adding 2 cm of shielding, the aperture of the first quadrupole should be 7.14 cm. The pole-tip field required will be 4.8 T only. The vertical chromaticity can be estimated to be

$$\xi_y = - \sum \frac{k\beta_y}{4\pi} \sim - \frac{s}{2\pi\beta_y^*} = -20 , \quad (4)$$

where the contribution of only one quadrupole has been included. Thus the total vertical chromaticity of the IR will be around  $-40$ , about one half of that in the lattice presented in Sec. I and II. The actual chromaticity should be much smaller, because the design has not been optimized. There will be cancellation of chromaticity between the F- and D-quadrupoles.

We would like to use two examples to give a better illustration. In the first example, the first quadrupole reverses  $\alpha_y$  to  $-\alpha_y$ , and the second quadrupole reverses  $\alpha_x$  to  $-\alpha_x$ . The thin-lens solution is given in Table 3. Whenever two values appear, the first one is at entrance of quadrupole and the second at exit. The integrated strengths of the first and second quadrupoles are  $k = +0.40$  and  $-0.75$  m $^{-1}$ , respectively. The chromaticities for the half IR are  $\xi_y = +3.98$  and  $\xi_x = -7.59$ .

In Example 2, we equalize the horizontal and vertical chromaticities and at the same time minimize them. We find that the two quadrupoles have integrated strengths of  $k = 0.4330$  and  $-0.5775$  m $^{-1}$ , respectively. The chromaticities for the half IR are  $\xi_x = \xi_y = -5.57$ . The Twiss properties at the quadrupoles are listed

in Table 4. Our results imply that the chromaticities of the whole IR with unequal  $\beta^*$ 's can be as low as  $\sim -12$ . Thus local correction at the IR will be unnecessary. We would like to point out, however, that the optimization of chromaticities made in this example does not necessarily be viewed as the best design of the lattice.

**TABLE 3.** Twiss properties of IR in Example 1.

$s$ (m)	0	5	6
$\beta_y$ (m)	0.04	625	400
$\alpha_y$	0	-125, +125	+100, -200
$\gamma_y$ (m <sup>-1</sup> )	25	25, 25	25, 99.7
$\beta_x$ (m)	0.40	62.9	161
$\alpha_x$	0	-12.5, -37.7	-60.2, +60.2
$\gamma_x$ (m <sup>-1</sup> )	2.5	2.50, 22.6	22.6, 22.6

**TABLE 4.** Twiss properties of IR in Example 2.

$s$ (m)	0	5	6
$\beta_y$ (m)	0.04	625	358
$\alpha_y$	0	-125, +152	+115, -91.9
$\gamma_y$ (m <sup>-1</sup> )	25	25, 36.9	36.9, 23.6
$\beta_x$ (m)	0.40	62.9	170
$\alpha_x$	0	-12.5, -40.4	-66.3, +33.6
$\gamma_x$ (m <sup>-1</sup> )	2.5	2.5, 25.9	25.9, 5.91

## V CONCLUSION

We have presented a lattice for the 50-50 GeV muon collider that entails a relatively large dynamical aperture. In order to further enlarge the dynamical aperture even in the presence of field errors and fringe-field effects, we propose to replace the FMC modules in the arc with FODO cells and modify the IP by having unequal horizontal and vertical betatron functions. The chromaticities will be much smaller making local correction unnecessary. With the FODO cells, 3 family of sextupoles can be deployed in each plane making the control of variation of  $\beta^*$ 's and chromaticities with momentum offset possible.

## REFERENCES

1. R. Palmer for the Muon Collider Collaboration, "Muon Collider: Introduction and Status," to be published in Proc. Workshop on Phys. at First muon Collider and at Front End of a Muon Collider, Fermilab, Batavia, November 6-9, 1997.
2. M. Donald, R. Helm, J. Irwin, H. Moshhammer, E. Forest, D. Robin, A. Zholents, and M. Sullivan, "Localized Chromaticity Correction of Low-Beta Insertions in Storage Rings," Proc. 1993 Part. Accel. Conf., Washington, D.C., May 17-20, 1993, pp. 131.
3. S.Y. Lee, K.Y. Ng, and D. Trbojevic, Phys. Rev. **E48**, 3040 (1993).
4. COSY INFINITY, a New Multipurpose Arbitrary Order Beam Dynamics Code, Lawrence Berkeley Laboratory Report LBL-28881, March, 1990. We would like to thank Dr. Weishi Wan to track the dynamical aperture.
5. Ref. 3 shows large dispersion function is required to attain large negative momentum compaction. For the missing-dipole scenario, large quadrupole gradients are required as is illustrated in D. Trbojevic and K.Y. Ng, "A Proton Driver for the Muon Collider Source with a Tunable Momentum Compaction Lattice," to be published in Proc. Part. Accel. Conf., Vancouver, BC, May 12-16, 1997.
6. N. Huang, to be published in Proc. ICFA Workshop on Beam Dynamics Issues for  $e^+e^-$  Factories, Frascati, Italy, October 20-25, 1997; H. Koiso, *ibid.*